Inovasi Kesehatan Global
Volume. 3 Nomor. 1 Februari 2026
e-ISSN : 3046-4625, p-ISSN : 3046-4706, Hal. 94-108
DOI: https://doi.org/10.62383/ikg.v3i1.2799
Tersedia: https://journal.lpkd.or.id/index.php/IKG

Preparation and Molecular Docking of Some Heterocyclic Compounds Containing Nitrogen and Oxygen Atoms

Saad Salem Jassim
Chemistry Department, College of Sciences, University of Kirkuk, Kirkuk, Iraq.

**Corresponding Author: saadsalem@uokirkuk.edu.iq*

Abstract. *Derivatives of substituted oxazol-5-one (1–3) and substituted oxazolo-isoxazole (4–6) were successfully synthesized through a multi-step reaction process. Initially, glycine was reacted with acetic anhydride to produce acetyl glycine as a key intermediate. This intermediate subsequently underwent a condensation reaction with various substituted benzaldehydes, leading to the formation of oxazol-5-one derivatives (1–3). In the final synthetic step, these oxazol-5-one derivatives were reacted with hydroxylamine hydrochloride to yield the corresponding oxazolo-isoxazole compounds (4–6). The chemical structures of all synthesized compounds were characterized and confirmed using Fourier Transform Infrared (FT-IR) spectroscopy and proton nuclear magnetic resonance (^{1}H NMR) spectroscopy. Furthermore, molecular docking studies were carried out to evaluate the potential biological interactions of the prepared compounds. Docking simulations were performed using PyRx software, while visualization and interaction analysis were conducted employing PyMOL and Discovery Studio. The combined experimental and computational approaches provide valuable insights into the structural properties and potential biological relevance of the synthesized compounds.*

Keywords: *Chemical Synthesis; Cyclization; Isoxazole; Molecular Docking; Oxazol.*

1. INTRODUCTION

Heterocyclic compounds are cyclic organic compounds containing at least one heteroatom. The most common heteroatoms are sulfur, oxygen, and nitrogen. Because of their ability to treat a wide range of illnesses, heterocyclic compounds are seen to be among the most significant classes of organic chemicals. Oxazolo-isoxazole is considered to be a heterocyclic compound that consists of two fused five-membered rings with three double bonds included. Each ring contains three carbon atoms, one nitrogen atom and one oxygen atom at positions 1,2 and 4,6. The structure of oxazolo-isoxazole depends on the type of fusion of the two hetero rings.

Oxazolo-isoxazole compounds, which combine oxazole and isoxazole rings via reaction of 4-(4- benzylidene)-2-methyloxazole-5-one with hydroxylamine hydrochloride, and their equivalents exhibit a wide range of biological activities, making them extremely significant groups of heterocyclic chemical compounds. Isoxazole has been clinically demonstrated to be excellent as an antibacterial, antifungal, and anti-inflammatory. anticancer, antitubercular, and antineoplastic drug based on a thorough review of the literature.

Naskah Masuk: 17 November 2025; Revisi: 18 Desember 2025; Diterima: 15 Januari 2026;
Tersedia: 19 Januari 2026

2. EXPERIMENTAL

Synthesis of N-acetyl glycine [6].

Glycine (7.5 g, 0.1mol) was dissolved in 30 ml of water in a 100 ml flask using a magnetic stirrer. Acetic anhydride (10 ml, 0.1 mole) was added in one portion with continuous stirring for 20 minutes. The solution becomes hot, and some N-acetyl glycine may crystallize. The reaction mixture was cooled in an icebox overnight, whereby a crystalline solid was precipitated, washed with ice-cold water, and dried. M.P. = 203-205, Yield% = 75, White.

Synthesis of Substituted Oxazol-5-one. [7,8]

To the mixture of N-acetyl glycine (4.68 g, 0.04 mole), substituted benzaldehyde (0.04 mol), and sodium sulphate (2.84 g, 0.02 mole), acetic anhydride (12 mL) was added. The mixture was refluxed for 6 hours, cooled, and left in the icebox overnight. 12 ml of water was added to the precipitate obtained, filtered, washed with cold water, dried, and crystallized from ethanol.

Table 1. Physical properties of compounds (1-3).

Com. No.	X	Structure Formula	Molecular Weight	M.P. ºC	Yield %	Color
1	H	$C_{11}H_9NO_2$	187	134-136 139-141*	67	Yellow
2	$(CH_3)_2N$	$C_{13}H_{14}N_2O_2$	230	68-70	87	Orange
3	OH	$C_{11}H_9NO_3$	203	110-113	78	Brown

Synthesis of Substitute Oxazolo[5,4-c]Isoxazole

Mixture of 5-(4-benzylidene-2-methyl-oxazole-5-one) (0.015 mol), hydroxylamine hydrochloride (1.04 g, 0.015 mol), and sodium acetate (1.23 g, 0.015 mol) was refluxed in ethanol for 7-8 hours. TLC tracked the completion of the reaction. After the solvent had been evaporated from the mixture at low pressure, the resulting solution was placed into cold water, filtered, and dried., and recrystallized from ethanol.

Table 2. Physical properties of compounds (4-6)**.**

Com. No.	X	Structure Formula	Molecular Weight	M.P. ºC	Yield %	Color
4	H	$C_{11}H_8N_2O_2$	200	134-136	78	White
5	$(CH_3)_2N$	$C_{13}H_{13}N_3O_2$	243	143-145	72	Yellowish white
6	OH	$C_{11}H_8N_2O_3$	216	211-213	85	Yellow

3. RESULTS and DISCUSSION

Identification of Compounds (1-3):

Compounds (1-3) were prepared by reacting acetyl glycine with p-substituted benzaldehyde in presence of in a basic medium as in the equation below:

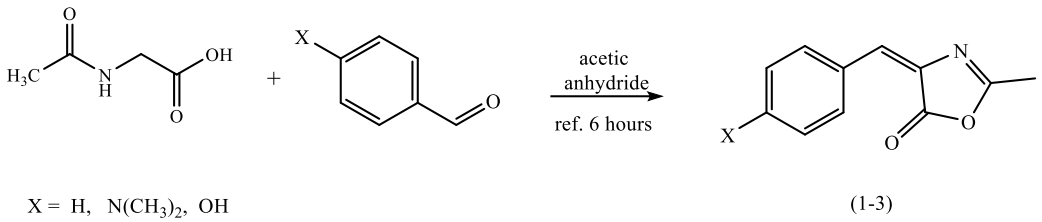

X = H, $N(CH_3)_2$, OH (1-3)

The reaction is believed to proceed according to the below mechanism:

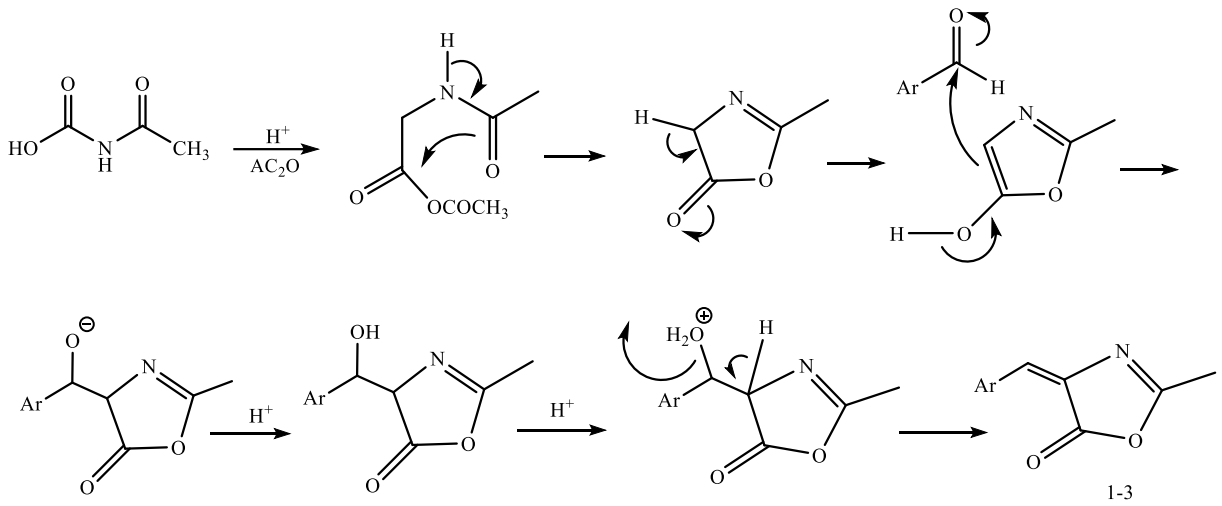

Ar = H, $(CH_3)_2N$, OH

Compounds (1-3) were characterized by the infrared spectrum, exhibiting absorption peaks in the range of 1469-1491 and 1592-1596 cm^{-1}, for the symmetrical and asymmetrical stretching frequency corresponding to the aromatic C=C bond. The stretching frequency of the C=N group (oxazolone ring) was observed as a strong to medium-intensity band in the range of 1640-1650 cm^{-1}. The stretching frequency of the C=O and absorption peaks within the range of 1752-1778 cm^{-1} for the C=O bond (oxazolone ring). Additionally, there were absorption peaks at 2866-2883 and 2942-2989 cm^{-1} for the symmetrical and asymmetrical stretching frequency of the aliphatic C-H bond, along with an absorption peak at 3035-3084 cm^{-1} for the aromatic C-H bond, Furthermore, the presence of a chemical reaction was suggested by the loss of absorption peaks linked to the symmetrical and asymmetrical absorption of the (NH_2) group is typical of hydrazide. Reference to Table 3 and figures. 1 and 2 were made.

Table 3. Infrared spectral data of compounds (1-3).

Com. No.	IR(KBr). ν (cm^{-1})						
	(C-H) aliphatic Sym. Asy.	(C-H) aromatic	(C=N)	(C=O) oxazolone	(C=C) Aromatic Sym. Asy	(C-O-C)	Other absorptions
1	2945 2866	3038	1649	1778	1489 1593	1071	-
2	2989 2881	3035	1650	1769	1491 1596	1072	-
3	2942 2883	3084	1640	1752	1469 1592	1225	(O-H) 3343

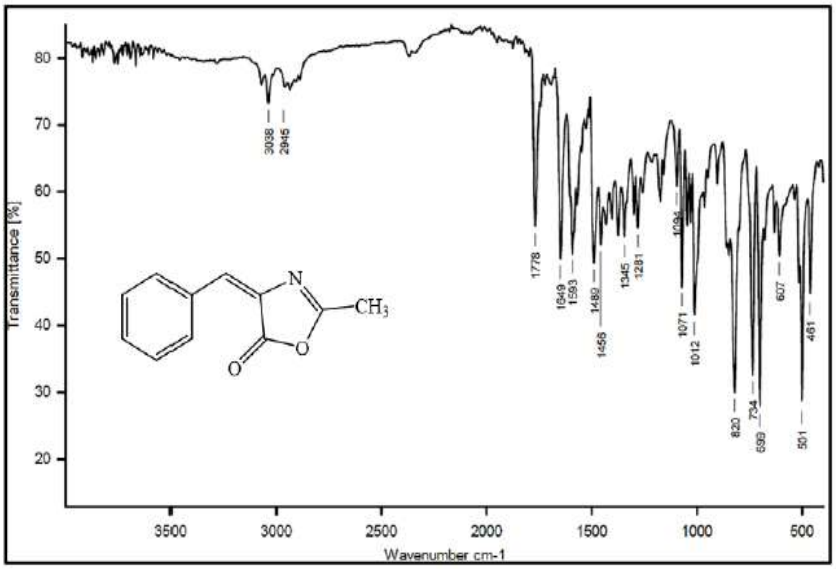

Figure 1. IR for compound (1).

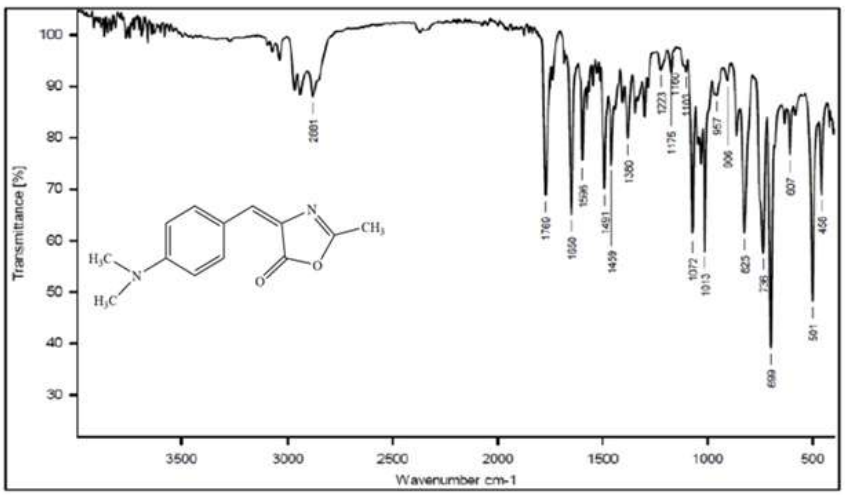

Figure 2. IR for compound (2).

The ^{1}H-NMR spectra revealed a change in the signals of the reactants, as well as the appearance of new signals consistent with the composition of the final products. The TMS reference signal was not observed due to its being set to zero when measured from the source.

^{1}H-NMR spectra of Compound (1) showed a singular signal at 1.82 ppm, assigned to the methyl (CH_3) protons. A single signal appeared at 7.55 ppm, attributed to the methine proton (=CH), with multiple signals ranging from 7.70 to 7.90 ppm, corresponding to the protons of the aromatic ring, as shown in figure 3.

^{1}H-NMR spectra of Compound (2) showed a singular signal at 2.2 ppm and 2.8 ppm assigned to the methyl (CH_3) protons and ((CH_3)$_2$N) group, the multiple singular signals at 6.8-8.5 ppm, attributed to the aromatic protons. While compound (3) showed a distinct signal at 1.90 ppm, attributed to the methyl (CH_3). The proton of the methine group =CH appeared as part of a multiplate along with several signals between (6.88-7.10) ppm, associated with the protons of the aromatic ring. Additionally, the OH group showed a signal at 8.68 ppm, as figure 4 illustrates.

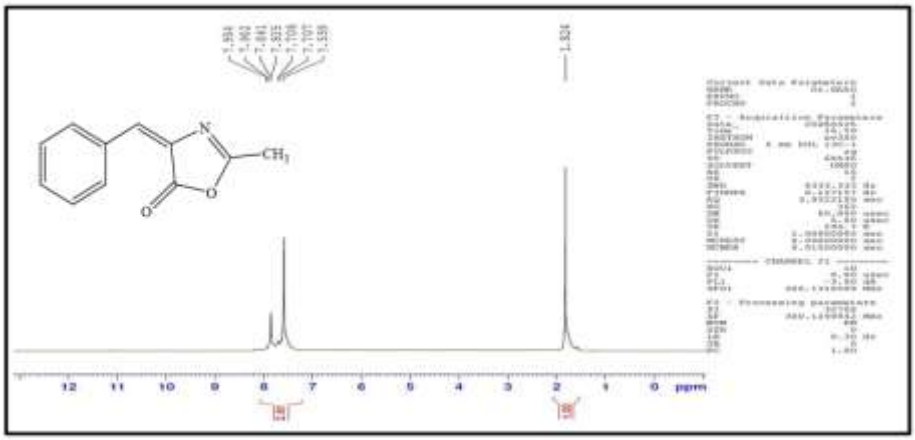

Figure 3. ^{1}H-NMR for compound (1).

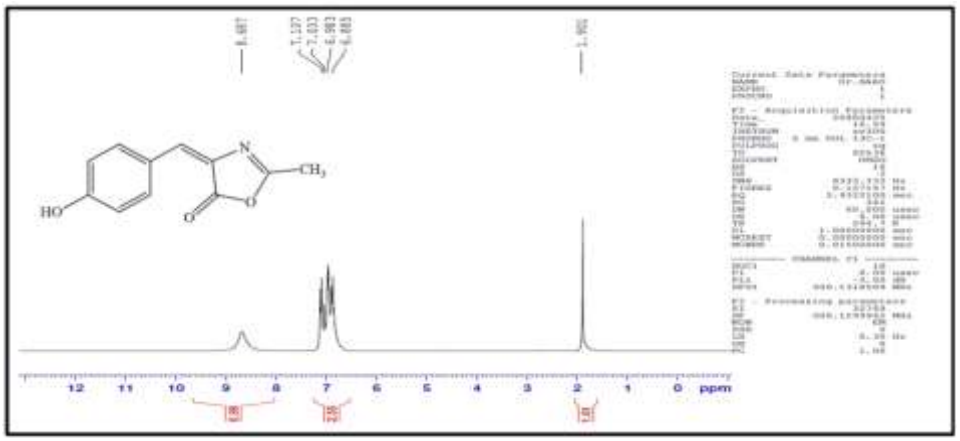

Figure 4. ^{1}H-NMR for compound (3).

Identification of Compounds (4-6)

Compounds (4-6) were prepared by reacting the compounds (1-3) with hydroxylamine hydrochloride in the presence of ethanol, as in the equation below:

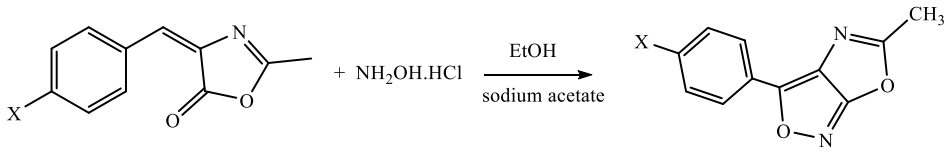

X= H, $(CH_3)_2N$, OH

The reaction is believed to proceed according to the below mechanism:

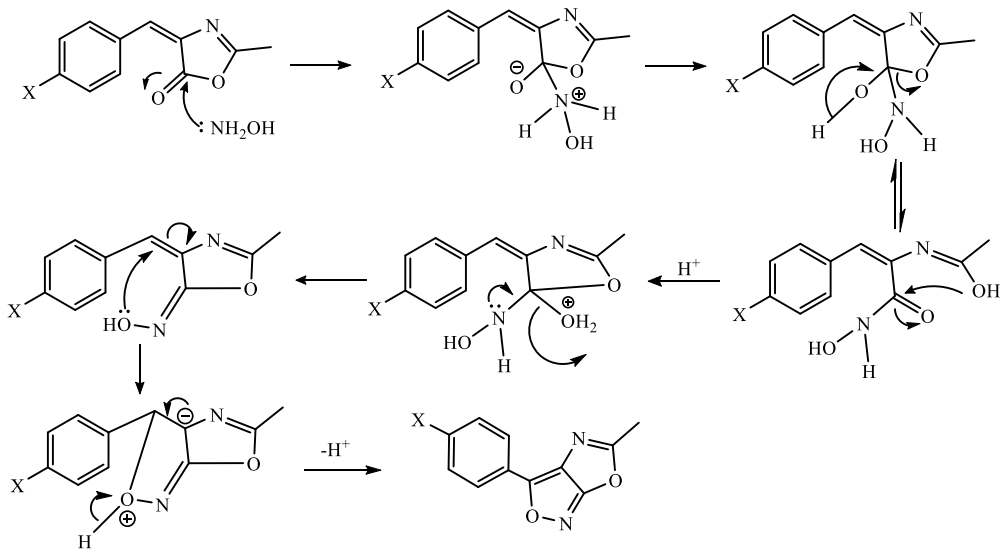

X= H, $(CH_3)_2N$, OH

The infrared spectra of the produced compounds (4-6) showed two absorption peaks that corresponded to aromatic C=C and fell between 1434-1494, and 1494-1596 cm^{-1}. The group (C=N) showed a high to medium-intensity stretching frequency that fell between 1602-1650 cm^{-1}, while the group (C-O-N of isoxazole) showed an absorption peak that fell between 1091-1269 cm^{-1}. Furthermore, the aliphatic C-H bond has an absorption peak at 2850-2860 and 2928-2900 cm^{-1} for the symmetrical and asymmetrical stretching frequency, while the aromatic C-H bond exhibits an absorption peak at 3039-3045 cm^{-1}. These results were in line with previous research. figures. 5, and 6, as well as Table 4, were noted.

Table 4. Infrared spectral data of compounds (4-6).

Com. No.	IR(KBr). ν (cm^{-1})					
	(C-H) aliphatic Sym. Asy.	(C-H) aromatic	(C=N)	(C=C) Aromatic Sym. Asy	(C-O-C)	Other absorptions
4	2900 2850	3039	1650	1457 1494	1091	-
5	2928 2860	3040	1602	1491 1596	1158	(C-N) 1269
6	2915 2856	3045	1638	1434 1567	1125	(O-H) 3292

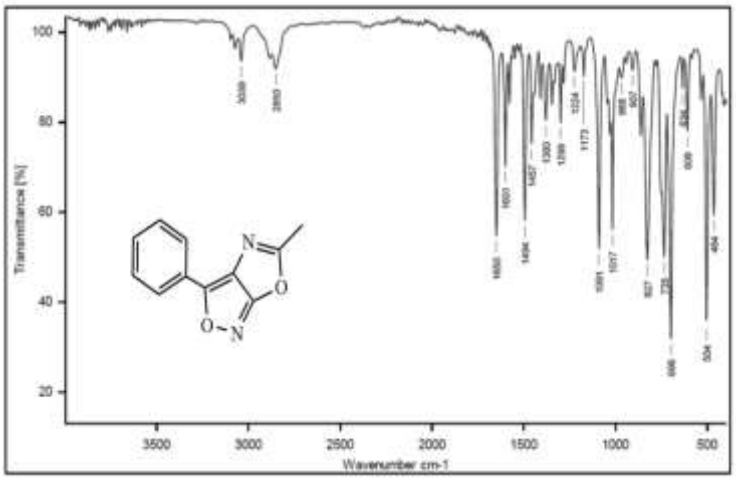

Figure 5. IR for compound (4).

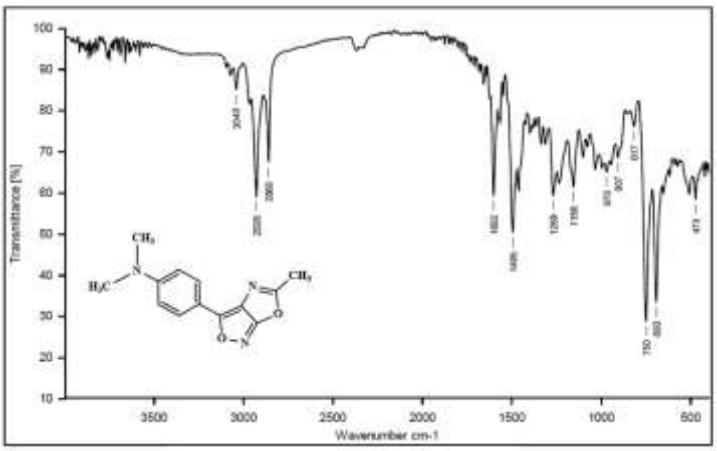

Figure 6. IR for compound (5).

The ^{1}H-NMR spectra of compound (4) revealed a separate signal at 2.90 ppm, corresponding to the methyl (CH_3) group. Phenyl rings provide several signals (7.14-7.85) ppm, as shown in figure 7**.**

Compound (5) ^{1}H-NMR spectra showed a distinct signal at 2.78 ppm, which is attributed to the protons of the methyl group (CH_3). A single signal also appeared at 3.02 ppm, which is attributed to the protons of the two methyl groups -$N(CH_3)_2$. The aromatic ring provides several signals (6.83-7.78) ppm, as shown in figure 8. For compound (6), the ^{1}H-NMR spectra showed a clear signal at 2.52 ppm, attributed to the protons of the methyl

group (CH_3). The aromatic ring provided several signals (7.82-8.20) ppm, and a single signal appeared at 10.10 ppm, attributed to the proton of the OH group, as shown in figure 9.

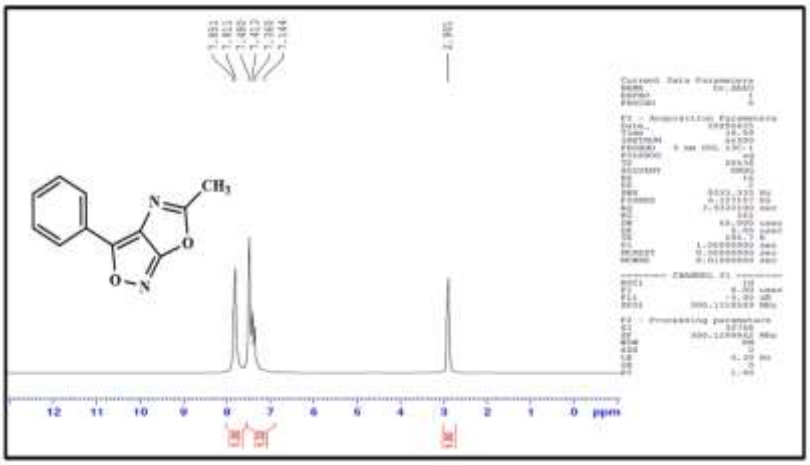

Figure 7. ^{1}H-NMR for compound (4).

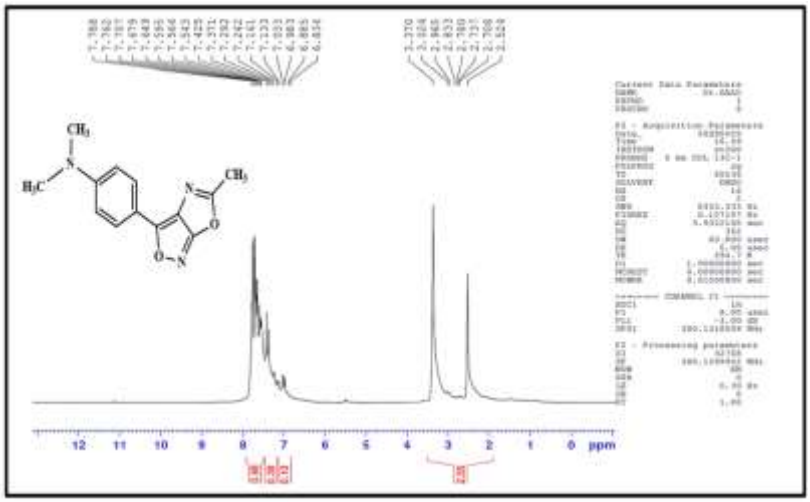

Figure 8. ^{1}HNMR for compound (5).

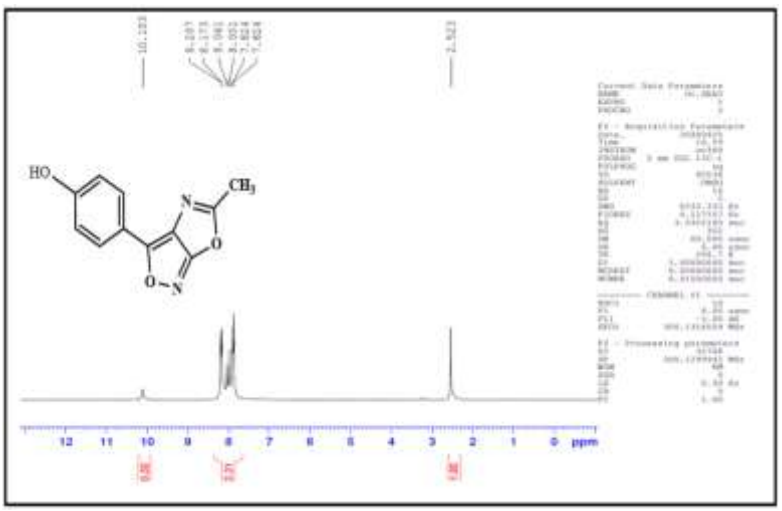

Figure 9. ^{1}H-NMR for compound (6).

4. MOLECULAR DOCKING OF THE PREPARED COMPOUNDS

The 7DPP SARS-CoV-2 3CL protease (3CLpro) crystal structures were retrieved from the Protein Database, whereas the structure was derived from the synthesized molecule. To further understand the interaction that occurred between the synthesized chemicals and the viral protein, the molecular docking simulation was conducted utilizing bioinformatics tools such as the Pyrex software. The Pyrex application was used to simulate docking. The produced compounds were docked with the 7DPP enzyme at the binding site. First constructed in Chem3d, the generated compounds (1- 6) were saved in a PDBQT input file for docking investigations. Importing the pertinent Protein Data Bank information and utilizing Pyrex to eliminate non-standard residues were necessary steps in the creation of 7DPP models.

After this configuration, Pyrex run in a grid box to examine and access the docking conformation. Pyrex analysis was performed using Pymol and Discover Studio. Visualizing the structures was the main goal of the Discover studio program. Pyrex software was used to reveal each drug and all of the protein's interacting residues. Molecular docking modeling is essential, especially for the screening of potential new medicinal compounds.

We compared the outcomes of our molecular docking models of chemicals with viral protein. Examine the produced compounds' potential as a new viral protein inhibitor. The examination of molecular docking results involving the chosen viral protein revealed the most promising enzyme displaying the best interaction with (1-6).

Protein residues that created H-bonds and other kinds of bonds with the chemical were displayed by the software. A higher number of hydrogen bonds suggests a higher complex binding affinity and a more robust connection between the chemical complex and protein. According to Discover Studio and Pymol, Table 5 shows the quantity of hydrogen bond forms, the interacting residues, and the interaction between the prepared compounds and the protein.

Results of Molecular Docking Studies

To determine the closeness of the target protein from bacterial species to all produced compounds, we used molecular docking (1-6). Ideal docking interaction scores were obtained by analyzing the 3FYV binding pockets; these scores, bond types, binding sites (1-4), active site amino acid residues, and the ability of derivatives to occupy different places are shown in Table 5. Docking experiments suggest that the prepared molecules may also possess antimicrobial qualities. The interactions between the synthetic chemical derivatives

and the amino acid residues found in 7DPP coli's active sites are depicted in both 2D and 3D in the pictures below.

Table 5. Interacting residues of protein with the prepared compound that were analyzed by Pyrex and Discover studio.

Com. No.	Binding Energy kcal/mol	Interaction residues
1	-4.3	ARG A:105, GLU A:178
2	-5.8	HIS A:172, HIS A:163, ASN A:142, MYC A:401, MET A:165
3	-6.2	GLY A:143, ASN A:142, CYS A:145, MYC A:401, GLU A:166
4	-6.4	GLY A:143, CYS A:145, MYC A:401
5	-6.3	ASN A:142, HIS A:172, HIS A:163, MYC A:401, GLY A:143, CYS A:145 SER A:144
6	-7.4	GLU A:166, HIS A:163, SER A:144, MYC A:401, GLY A:143

As Table 4 illustrates, a complex's binding energy indicates whether the binding is stable or unstable. A positive binding energy indicates steady binding. The findings showed that all complexes had negative binding energy values, indicating that the complex's binding had stabilized and that the compounds generated were suitable for the particular binding site of the 7DPP protein. Furthermore, the binding energies of compounds 1, 2, 3, 4, 5, and 6 were (-4.3, -5.8, -6.2, -6.3 and-7.4), respectively, as demonstrated by molecular docking simulations. With the exception of the 7DPP-6 and 7DPP-1 complexes, all of the compounds' binding energy values were quite comparable.

Because there was no hydrogen bond contact between 1 and 7DPP, the interaction was weak for the 7DPP-1 complex. The 7DPP-6 combination is the best ligand to form a complex with the 7DPP protein since it has the lowest binding energy value. This is due to the fact that the binding affinity, which is higher when the binding energy value is lower, indicates the strength of the binding interaction between the protein and ligand complex. This is due to the fact that the binding affinity, which is higher when the binding energy value is lower, indicates the strength of the binding interaction between the protein and ligand complex.

The interaction between the synthesized chemical and the 7DPP protein with 2D and 3D formation is depicted in Figures 10, 11, 12, 13, 14, and 15, along with the many forms of potential bonding with the protein. The compound (6) had the best interaction, while the compound (1) had the worst, as seen in the figures10 and 15 and Table 5.

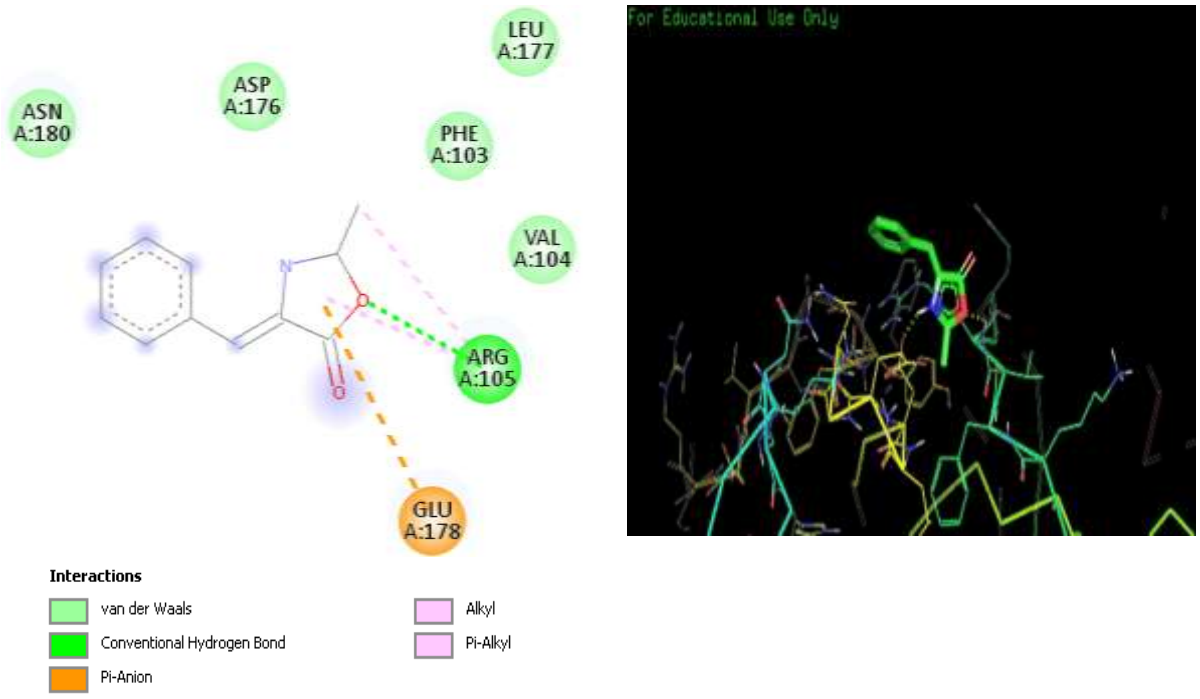

Figure 10. The interaction between compound (1) and the 7DPP protein.

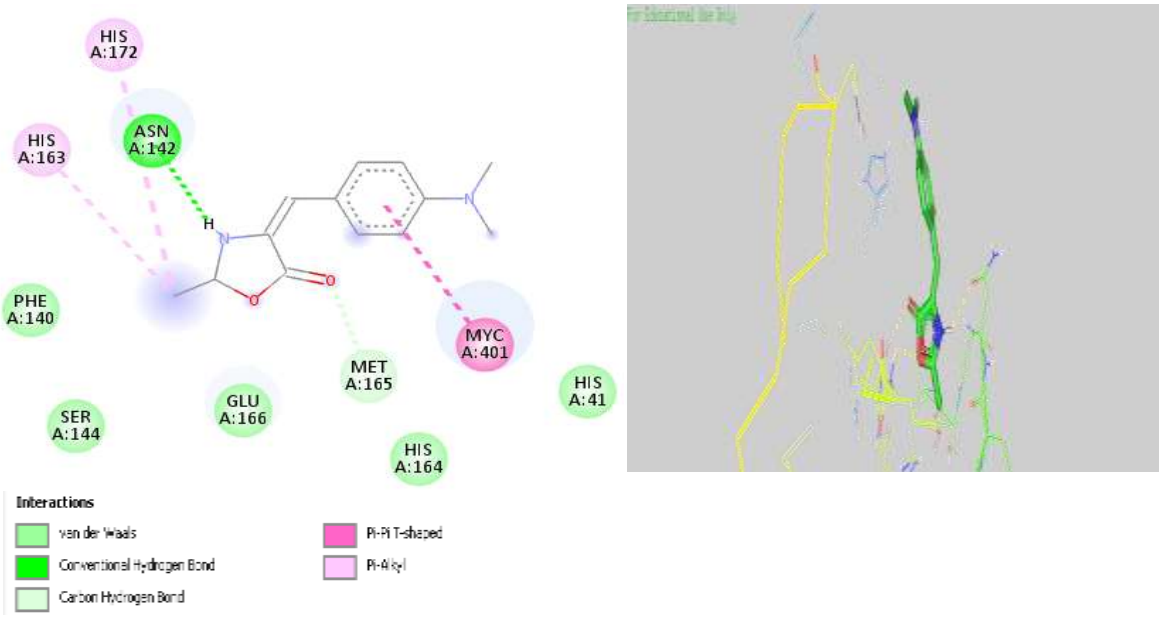

Figure 11. The interaction between compound (2) and the 7DPP protein

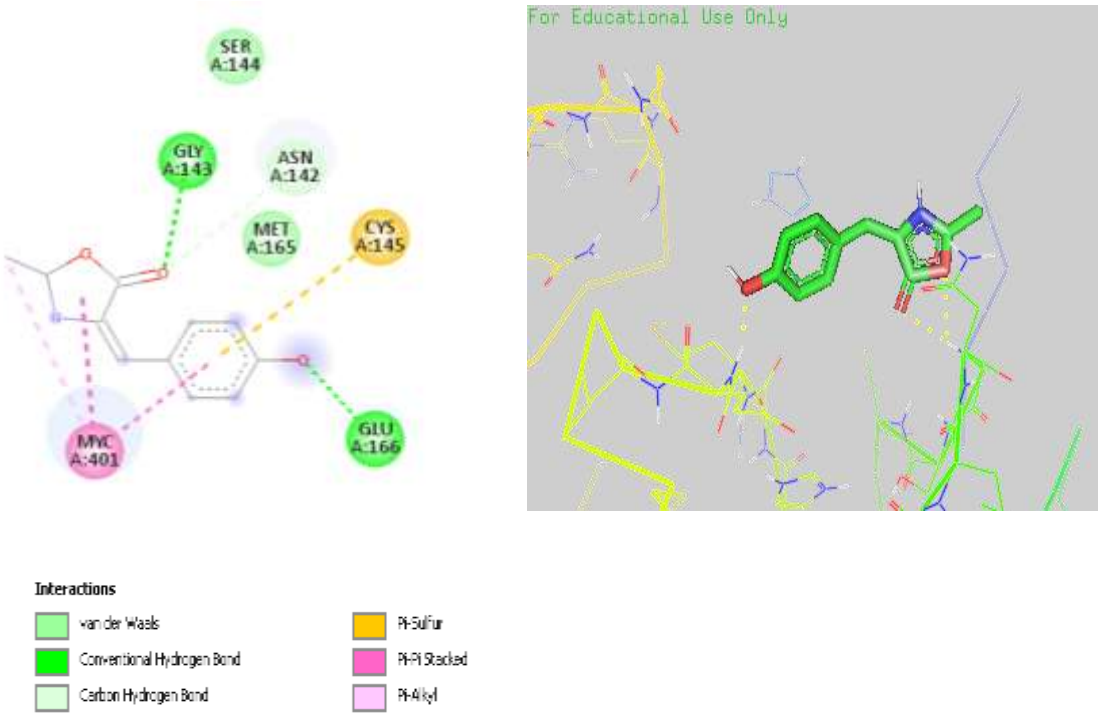

Figure 12. The interaction between compound (3) and the 7DPP protein.

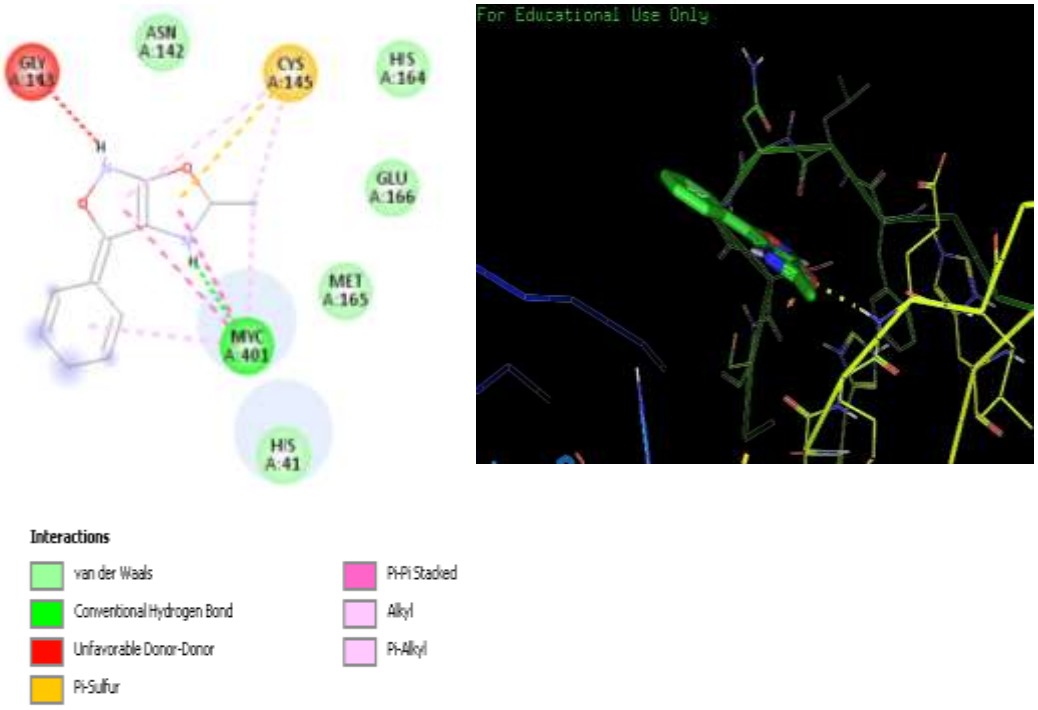

Figure 13. The interaction between compound (4) and the 7DPP protein.

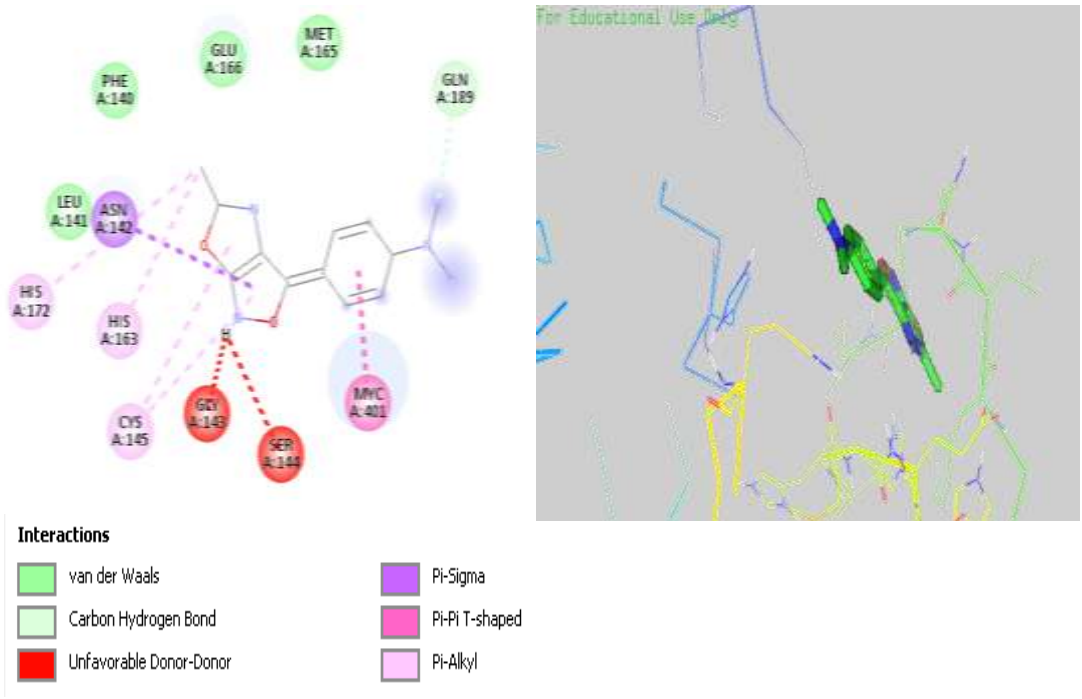

Figure 14. The interaction between compound (5) and the 7DPP protein.

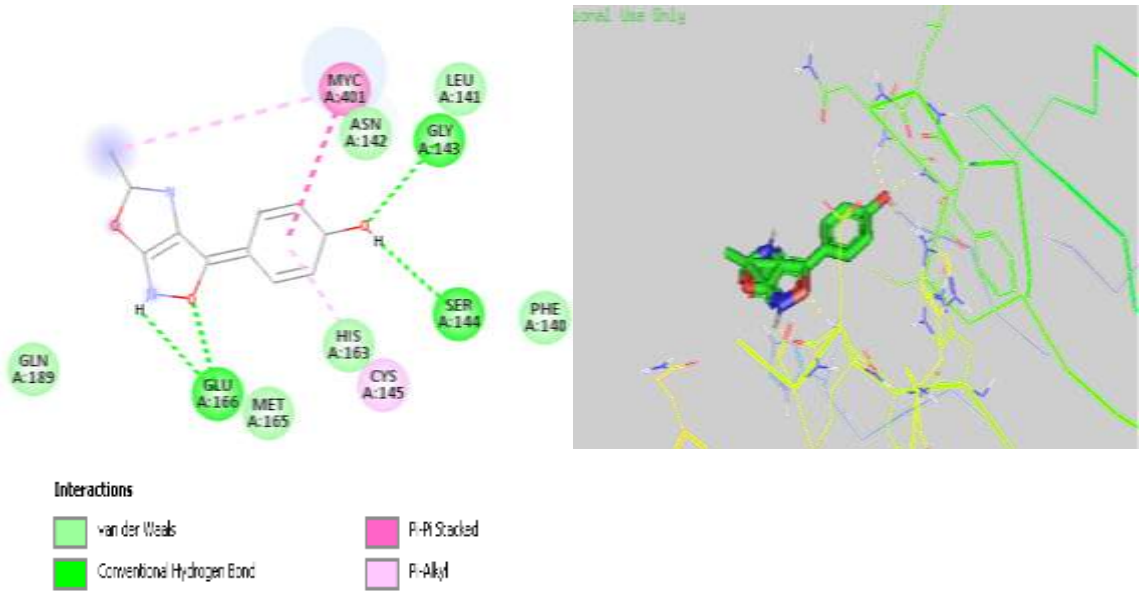

Figure 15. The interaction between compound (6) and the 7DPP protein.

5. CONCLUSIONS

The formulations' high purity and advantageous yield were confirmed by FT-IR and ^{1}H-NMR spectroscopy. Because there was no hydrogen bond contact between compound (1) and 7DPP, the interaction was weak for the 7DPP-1 complex. The 7DPP-6 combination is the best ligand to form a complex with the 7DPP protein since it has the lowest binding

energy value. This is due to the fact that the binding affinity, which is higher when the binding energy value is lower, indicates the strength of the binding interaction between the protein and ligand complex. This is due to the fact that the binding affinity, which is higher when the binding energy value is lower, indicates the strength of the binding interaction between the protein and ligand complex**.**

The interaction between the synthesized chemical and the 7DPP protein with 2D and 3D formation is depicted in Figures 10, 11, 12, 13, 14, and 15, along with the many forms of potential bonding with the protein. The compound (6) had the best interaction, while the compound (1) had the worst.

REFERENCES

Agrawal, N., & Mishra, P. (2018). The synthetic and therapeutic expedition of isoxazole and its analogs. *Medicinal Chemistry Research, 27*(5), 1309–1344. https://doi.org/10.1007/s00044-018-2152-6

Al-Tufah, M. M., Beebaeny, S., Jasim, S. S., & Mohammed, B. L. (2023). Synthesis and characterization of ethyl dioxoisoindolinyl cyclohexenone carboxylate derivatives from some chalcones and its biological activity assessment. *Chemical Methodologies, 7*, 408–418. https://doi.org/10.22034/CHEMM.2023.388126.1654

Cazzaniga, G., Tresoldi, A., Gelain, A., Meneghetti, F., Mori, M., & Villa, S. (2024). Eco-friendly bio-based solvents for the acetylation of the amino group of amino acids. *Chemistry & Biodiversity, 21*(2), e202301729. https://doi.org/10.1002/cbdv.202301729

Dudik, A. S., Zanakhov, T. O., Galenko, E. E., Novikov, M. S., & Khlebnikov, A. F. (2025). Azirinyl-substituted nitrile oxides: Generation and use in the synthesis of isoxazole-containing heterocyclic hybrids. *Molecules, 30*(13), Article 2834. https://doi.org/10.3390/molecules30132834

Gujjarappa, R., Sravani, S., Kabi, A. K., Garg, A., Vodnala, N., Tyagi, U., & Malakar, C. C. (2022). An overview on biological activities of oxazole, isoxazoles and 1,2,4-oxadiazoles derivatives. In *Nanostructured biomaterials: Basic structures and applications* (pp. 379–400). Springer. https://doi.org/10.1007/978-981-16-8399-2_10

Jasim, S. S., Abdulwahid, J. H., Beebany, S., & Mohammed, B. L. (2023). Synthesis, identification, and antibacterial effect assessment of some new 1,4-thiazepines derived from substituted diphenyl acrylamides and diphenyl dienones. *Chemical Methodologies, 7*, 509–523. https://doi.org/10.22034/CHEMM.2023.392659.1668

Jassim, S. S. (2019). Preparation and identification of Schiff bases (1,3-oxazepine or diazepine-7,4-dione) and evaluation of their antibacterial activity. *Kirkuk Journal of Science, 14*(2), 249–272. https://doi.org/10.32894/kujss.2019.14.2.15

Jassim, S. S. (2019). Synthesis and characterization of some bis-1,3-oxazepine-4,7-dione and 1,3-diazepine-4,7-dione derivatives. *Kirkuk Journal of Science, 13*(2), 149–165. https://doi.org/10.32894/kujss.2018.145725

Jayasinghe, R. N., Padukkage Dona, N. T., Lorensu Hewage, V. C., Egodawaththa, N. M., Nesnas, N., & Gunaratna, M. J. (2025). Evaluation of in silico and in vitro antidiabetic properties of 4-(hydroxysubstituted arylidene)-2-phenyloxazol-5(4H)-one derivatives. *ACS Omega, 10*(8), 8009–8022. https://doi.org/10.1021/acsomega.4c09061

Jirjees, I. (2022). Design and characterization of oxazepine new derivatives. *International Journal of Health Sciences, 6*(S2), 7380–7387. https://doi.org/10.53730/ijhs.v6nS2.6710

Kakkar, S., & Narasimhan, B. (2019). A comprehensive review on biological activities of oxazole derivatives. *BMC Chemistry, 13*(1), Article 16. https://doi.org/10.1186/s13065-019-0531-9

Khalaf, H. M. M., Gouda, M., Amer, A. A., Abdelhamid, A. A., & Abdou, A. (2024). Design and synthesis of new mixed azo-hydroxyquinoline complexes: In vitro anti-inflammatory, antifungal, antibacterial, theoretical, and molecular docking interactions investigation. *Journal of Molecular Structure, 1307*, Article 138016. https://doi.org/10.1016/j.molstruc.2024.138016

Nariya, P., Patel, M., & Thakore, S. (2024). *Synthesis, mesomorphic properties, and DFT calculations of curcumin-oxazole modified Schiff base liquid crystals* [Manuscript]. SSRN. https://ssrn.com/abstract=4921559

Nguyen, C. T., Dinh, D. T. H., Van Nguyen, T., Le, G. D., & Nguyen, H. C. (2019). Synthesis and antimicrobial activity of some 1-arylideneamino-4-(4-chlorobenzylidene)-2-methyl-1H-imidazolin-5(4H)-one compounds. *Oriental Journal of Chemistry, 35*(2), 822–829. https://doi.org/10.13005/ojc/350245

Potkin, V., Petkevich, S., Kletskov, A., Dikusar, E., Zubenko, Y. S., Zhukovskaya, N., & Pashkevich, S. (2013). Synthesis of functionally substituted isoxazole and isothiazole derivatives. *Russian Journal of Organic Chemistry, 49*(10), 1523–1533. https://doi.org/10.1134/S1070428013100205

Rani, A., Khan, J., Aslam, M., Ali, A., Kamthan, M., Pandey, G., & Nand, B. (2025). Design, synthesis, and biological evaluation of Schiff-base isoxazole hybrids: Exploring novel antimicrobial agents. *Bioorganic Chemistry, 159*, Article 108428. https://doi.org/10.1016/j.bioorg.2025.108428

Sahoo, M., Sahoo, B., Panda, J., & Kumar, A. (2017). Microwave-induced synthesis of substituted isoxazoles as potential antimicrobial agents. *Current Microwave Chemistry, 4*(2), 146–151. https://doi.org/10.2174/2213335603666160926101734

Vashisht, K., Sethi, P., Bansal, A., & Bansal, P. (2025). Antimicrobial activity of isoxazole derivatives: A brief overview. *Vietnam Journal of Chemistry, 63*(2), 195–213. https://doi.org/10.1002/vjch.202400029

Walunj, Y., Mhaske, P., & Kulkarni, P. (2021). Application, reactivity and synthesis of isoxazole derivatives. *Mini-Reviews in Organic Chemistry, 18*(1), 55–77. https://doi.org/10.2174/1570193X17999200511131621